AGU PUBLICATIONS

JGR

Journal of Geophysical Research: Oceans

RESEARCH ARTICLE

10.1002/2016JC012335

Nitrogen fixation in the eastern Atlantic reaches similar levels in the Southern and Northern Hemisphere

Debany Fonseca-Batista [1], Frank Dehairs [1], Virginie Riou [2], François Fripiat[1,3], Marc Elskens[1], Florian Deman [1], Natacha Brion [1], Fabien Quéroué[4], Maya Bode[5], and Holger Auel[5]

[1]Analytical, Environmental and Geo-Chemistry, Earth System Sciences Research Group, Vrije Universiteit Brussel, Brussels, Belgium, [2]Aix-Marseille Université, CNRS/INSU, Université de Toulon, IRD, Mediterranean Institute of Oceanography (MIO) UM 110, 13288, Marseille, France, [3]Now at Max Planck Institute for Chemistry, Mainz, Germany, [4]LEMAR-UMR 6539, CNRS-UBO-IRD-IFREMER, Plouzané, France, [5]Bremen Marine Ecology, Marine Zoology, University of Bremen, Bremen, Germany

Key Points:
- Widespread biological N2 fixation in the eastern Atlantic Ocean between 38°N and 21°S
- Comparable levels in the South and North East Atlantic
- Reassessment of annual nitrogen input through N2 fixation in the Atlantic Ocean

Supporting Information:
- Supporting Information S1
- Table S1
- Data Set S1

Correspondence to:
D. Fonseca-Batista,
dbatista8@hotmail.com

Citation:
Fonseca-Batista, D., F. Dehairs, V. Riou, F. Fripiat, M. Elskens, F. Deman, N. Brion, F. Quéroué, M. Bode, and H. Auel (2017), Nitrogen fixation in the eastern Atlantic reaches similar levels in the Southern and Northern Hemisphere, *J. Geophys. Res. Oceans*, *122*, 587–601, doi:10.1002/2016JC012335.

Received 13 SEP 2016
Accepted 9 DEC 2016
Accepted article online 22 DEC 2016
Published online 27 JAN 2017

Abstract Euphotic layer dinitrogen (N_2) fixation and primary production (PP) were measured in the eastern Atlantic Ocean (38°N–21°S) using $^{15}N_2$ and ^{13}C bicarbonate tracer incubations. This region is influenced by Saharan dust deposition and waters with low nitrogen to phosphorus (N/P) ratios originating from the Subantarctic and the Benguela upwelling system. Depth-integrated rates of N_2 fixation in the north (0°N–38°N) ranged from 59 to 370 μmol N m^{-2} d^{-1}, with the maximal value at 19°N under the influence of the northwest African upwelling. Diazotrophic activity in the south (0°S–21°S), though slightly lower, was surprisingly close to observations in the north, with values ranging from 47 to 119 μmol N m^{-2} d^{-1}. Our North Atlantic N_2 fixation rates correlate well with dust deposition, while those in the South Atlantic correlate strongly with excess phosphate relative to nitrate. There, the necessary iron is assumed to be supplied from the Benguela upwelling system. When converting N_2 fixation to carbon uptake using a Redfield ratio (6.6), we find that N_2 fixation may support up to 9% of PP in the subtropical North Atlantic (20°N–38°N), 5% in the tropical North Atlantic (0°N–20°N), and 1% of PP in the South Atlantic (0°S–21°S). Combining our data with published data sets, we estimate an annual N input of 27.6 ± 10 Tg N yr^{-1} over the open Atlantic Ocean, 11% of which enters the region between 20°N and 50°N, 71% between 20°N and 10°S, and 18% between 10°N and 45°S.

1. Introduction

Biological dinitrogen fixation (N_2 fixation) has been widely recognized as the dominant source of new nitrogen to the global ocean, with minor though significant contributions from riverine and atmospheric inputs [*Gruber and Sarmiento*, 1997; *Codispoti*, 2007; *Gruber*, 2008]. In tropical and subtropical regions where nitrogen (N) availability limits primary productivity, microbial N_2 fixation introducing new N to surface waters indeed plays a critical role in the net sequestration of carbon dioxide (CO_2) into the deep ocean [*Mahaffey et al*., 2005].

The magnitude of the global N input through N_2 fixation, however, has long been debated, and today significant uncertainties persist mainly related to limited spatial coverage of observations [*Luo et al*., 2012] as well as methodological issues [*Großkopf et al*., 2012]. Estimates for the global ocean based on geochemical parameters tend to converge to a range between 100 and 150 Tg N yr^{-1} [*Gruber and Sarmiento*, 1997, 2002; *Codispoti et al*., 2001; *Codispoti*, 2007; *Deutsch et al*., 2007]. The compilation of worldwide in situ measurements published by *Luo et al*. [2012] yields an annual input ranging between 62 and 137 Tg N yr^{-1}. The latter compilation however, included few data from regions such as the Indian Ocean, the South Pacific, and South Atlantic, and was mostly based on measurements carried out using the $^{15}N_2$ gas bubble-addition technique [*Montoya et al*., 1996].

The bubble-addition technique consists in injecting $^{15}N_2$ gas directly in the sample incubation bottle in order to follow its incorporation into the particulate matter. However, laboratory experiments [*Mohr et al*., 2010] and field measurements [*Großkopf et al*., 2012; *Wilson et al*., 2012; *Benavides et al*., 2013a; *Shiozaki et al*., 2015] have shown that in some cases direct bubble injection can underestimate the N_2 fixation rate

when compared to the "dissolution method," whereby the $^{15}N_2$ tracer is predissolved in a seawater aliquot before being added to the sample.

Based on the observed differences between N_2 fixation results obtained via the bubble-addition and the dissolution methods, *Großkopf et al*. [2012] estimated that global N_2 fixation may reach up to 177 Tg N yr^{-1} when considering only results obtained with the dissolution method. Since field measurements are best fit for a detailed understanding of the key role of N_2 fixation in the marine N cycle [*Gruber*, 2008], it appears important to contribute to the current database in order to better constrain global-scale estimates of N input.

The Atlantic Ocean is known to harbor substantial year-round diazotrophic activity [e.g., *Capone et al*., 2005; *Fernández et al*., 2010; *Sohm et al*., 2011a] accounting for ~25% of N_2 fixation in the global ocean [*Luo et al*., 2012]. It is therefore a key system for the global ocean N cycle.

The eastern North Atlantic in particular has been intensively studied [*Falcón et al*., 2004; *Voss et al*., 2004; *Capone et al*., 2005; *Montoya et al*., 2007; *Goebel et al*., 2010; *Benavides et al*., 2011, 2013a, 2013b; *Rijkenberg et al*., 2011; *Turk et al*., 2011; *Fernández et al*., 2013; *Painter et al*., 2013; *Schlosser et al*., 2014; *Snow et al*., 2015] since this region is under the influence of high nutrient input (e.g., iron and phosphate) through Saharan dust deposition known to stimulate N_2 fixation [*Mills et al*., 2004; *Langlois et al*., 2012]. Since iron (Fe) is a cofactor of the nitrogenase enzyme responsible for N_2 fixation [*Raven*, 1988], its availability may determine the distribution and intensity of N_2 fixation in the North Atlantic Ocean [*Paerl et al*., 1987; *Berman-Frank et al*., 2001], in conjunction with phosphorus (P) availability [*Mills et al*., 2004; *Langlois et al*., 2012].

South Atlantic regions and in particular the southeast Atlantic has attracted much less sampling efforts [*Staal et al*., 2007; *Moore et al*., 2009; *Fernández et al*., 2010; *Mouriño-Carballido et al*., 2011; *Sohm et al*., 2011b; *Großkopf et al*., 2012; *Snow et al*., 2015; *Wasmund et al*., 2015]. This basin has in fact long been considered to contribute little to global N_2 fixation, due to limited Fe availability. However the Benguela upwelling system (BUS) can carry dissolved metals from southern African shelves toward the gyre [*Noble et al*., 2012]. In addition, the BUS can also transport low nitrogen to phosphorus (N/P) signatures formed locally via denitrification and/or anammox [*Kuypers et al*., 2005; *Nagel et al*., 2013; *Flohr et al*., 2014]. Thereby significant N_2 fixation activity could potentially be sustained in the eastern South Atlantic [*Deutsch et al*., 2007; *Moore et al*., 2009; *Straub et al*., 2013].

The present study was carried out along a meridional transect through the eastern Atlantic Ocean, offering the possibilities (i) to cover the eastern South Atlantic region, notably undersampled for N_2 fixation activity [*Staal et al*., 2007; *Sohm et al*., 2011b; *Snow et al*., 2015; *Wasmund et al*., 2015] and (ii) to directly compare the activity between the North and South Atlantic regions which differ significantly in terms of dust input, a major factor controlling N_2 fixation. The specific aims of the study are (i) to investigate N_2 fixation over an extended latitudinal scale using the $^{15}N_2$ dissolution method, (ii) to assess its contribution to euphotic layer primary production (PP) and (iii) to evaluate the basin-wide annual N input from N_2 fixation.

2. Materials and Methods

Field observations were carried out between 1 and 24 November 2012 in the eastern Atlantic Ocean along a transect from 38°N to 21°S on board R/V Polarstern (ANT XXIX/1 EUROPA expedition, Figure 1). Samples were collected at 14 stations using a CTD (conductivity-temperature-depth) rosette system equipped with 24-Niskin bottles, a fluorescence sensor (WET Labs ECO-AFL/FL), and a photosynthetically active radiation sensor (PAR, PNF-300, Biospherical Instruments Inc.). Seawater was sampled from the surface down to 700 m to characterize the physical structure of the upper water column and associated biogeochemical properties (i.e., nutrients and oxygen). Ammonium (NH_4^+) and phosphate (PO_4^{3-}) concentrations were measured on board using standard fluorometric [*Holmes et al*., 1999] and colorimetric methods [*Grasshoff et al*., 1983] with detection limits (DL) of 44 and 42 nmol L^{-1}, respectively. Seawater dedicated to nitrate + nitrite ($NO_3^- + NO_2^-$) analysis was filtered over 0.2 μm pore size acrodiscs and stored at −20°C until analysis at the home-based laboratory. $NO_3^- + NO_2^-$ were analyzed according to *Grasshoff et al*. [1983] using a continuous flow QuAAtro autoanalyzer (Seal Analytical) with a DL of 80 nmol L^{-1}. Using our nutrient data, we calculated the excess PO_4^{3-}, P* as $= [PO_4^{3-}] - [NO_3^-]/16$ [*Deutsch et al*., 2007]. P* values were omitted when either ($NO_3^- + NO_2^-$) or PO_4^{3-} concentrations were below DL.

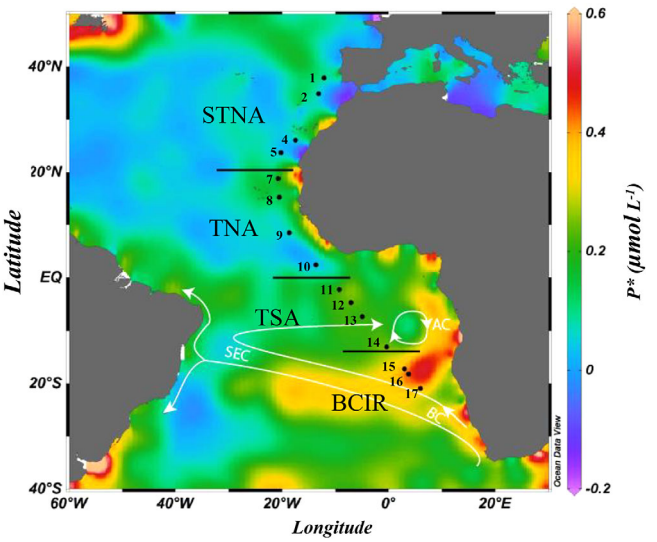

Figure 1. Location of stations during the ANT XXIX/1 EUROPA cruise (November 2012) superimposed on a map of seasonal average phosphate excess ($P^* = [PO_4^{3-}] - [NO_3^-]/16$) at 20 m depth (October–December from 1955 to 2012; World Ocean Atlas 2013) [*Garcia et al.*, 2013]. Crossed oceanographic provinces are indicated: subtropical North Atlantic (STNA), tropical North Atlantic (TNA), tropical South Atlantic (TSA), and Benguela Current-influenced region (BCIR). White arrows indicate surface currents in the eastern South Atlantic: Benguela Current (BC), South Equatorial Current (SEC), and Angola Current (AC) as adapted from *Peterson and Stramma* [1991].

2.1. Incubation Experiments

Isotopic tracer incubations were used for the simultaneous assessment of daily PP ($H^{13}CO_3^-$) and N_2 fixation ($^{15}N_2$) rates. Seawater was collected at depths equivalent to 50, 15, 3.5, and 0.5% of surface PAR in acid-cleaned polycarbonate (PC) bottles. All incubations lasting 24 h were performed in on-deck incubators flushed with surface seawater and wrapped with blue neutral density screens (Rosco) simulating the photometric depths. N_2 fixation was measured using the $^{15}N_2$ dissolution incubation method [*Mohr et al.*, 2010; *Großkopf et al.*, 2012] in duplicate at the four selected PAR levels (except for stations 1 and 14–17, where experiments were not duplicated). Briefly, $^{15}N_2$-enriched seawater was prepared by degassing, in acid-cleaned conditions, prefiltered (0.2 μm) low nutrient seawater (natural Sargasso Sea surface water purchased from OSIL), subsequently collected in 2 L gastight polypropylene Tedlar bags (Sigma-Aldrich). These bags were then injected with 30 mL of pure $^{15}N_2$ gas (98%+ ^{15}N, Eurisotop, lot number 23/051301) and shaken for equilibration of the tracer.

Details about the OSIL seawater, including its source region, nutrients and trace metals contents are presented in supporting information (Text S1), together with the results of our $^{15}N_2$ gas tests checking for potential contamination with ^{15}N-labeled substrates ($^{15}NO_3^-$, $^{15}NO_2^-$, and $^{15}NH_4^+$) [*Dabundo et al.*, 2014]. These background tests indicated that the applied protocol for N_2 fixation measurement was free of bias.

Prior to incubation, PC bottles (4.5 L) partially filled with sampled seawater were amended with approximately 250 mL of $^{15}N_2$-enriched seawater and spiked with 3 mL of 200 μmol L^{-1} $NaH^{13}CO_3$ (99% ^{13}C, Eurisotop) for PP assessment [*Hama et al.*, 1983]. Finally, incubation bottles were topped off with the original seawater sample and closed with a gas tight septum screw cap.

2.2. Uptake Rates Measurements

2.2.1. Laboratory Measurements and Computation

Rates were computed by measuring isotopic tracer enrichments in the organic matter at termination of the incubations [*Dugdale and Wilkerson*, 1986], as follows:

$$\text{Uptake rate} = \frac{Æ_{particle}^{final}}{Æ_{substrate}} \times \frac{[Particle]}{\Delta t} \left(\mu\text{mol m}^{-3}\ \text{d}^{-1}\right) \quad (1)$$

$Æ$ represents the atom percent (atom%) excess enrichment, i.e., ambient minus initial isotope abundances (^{15}N or ^{13}C atom%) of the substrate ($Æ_{substrate} = A_{substrate} - A_{particle}^{t=0}$) and the particulate matter ($Æ_{particle}^{final} = A_{particle}^{final} - A_{particle}^{t=0}$). [*Particle*] is the particulate nitrogen (PN) or particulate organic carbon (POC) concentrations after incubation (μmol L^{-1}) and Δt the incubation duration (days). $A_{substrate}$ is the ^{15}N% or ^{13}C% enrichment of dissolved N_2 gas or dissolved inorganic carbon (DIC), determined at the end of the incubation based on the assumption that 24 h $^{15}N_2$ and $H^{13}CO_3^-$ fixation activities do not significantly affect these large pools.

We used poisoned ($HgCl_2$) 12 mL Exetainers vials (Labco) to collect sample aliquots to measure these isotopic enrichments of dissolved N_2 and DIC substrates. Exetainers vials were then injected with helium (99.999%, Linde) to create a headspace and allow equilibration between gaseous and aqueous phases with or without addition of phosphoric acid (99%, Sigma-Aldrich) for DIC and N_2 analyses, respectively. Sample gas (N_2 or CO_2) was injected using a custom made manual gas injection port connected to the isotope ratio mass spectrometer (IRMS, Delta V, Thermo) via an Elemental Analyzer (Flash EA112, EA-IRMS). Measurements for DIC were corrected for gas partitioning and fractionation between dissolved and gaseous phase according to *Miyajima et al*. [1995]. $^{15}N_2$ enrichments were calibrated with atmospheric N_2 injections.

Incubation POC and PN concentration ([*Particle*]) and isotopic composition ($A^{final}_{particle}$ and $A^{t\,=\,0}_{particle}$) were assessed by filtering 4.5 L of samples onto precombusted MGF filters (glass microfiber filters, 25 mm diameter, 0.7 μm, Sartorius). Natural POC and PN concentration and isotopic composition were assessed by filtering nonspiked 4.5 L of seawater from each depth. POC and PN measurements were done using the method described by *Savoye et al*. [2004] on an EA-IRMS (Flash EA112, Delta V Plus, Thermo Scientific). The associated DL for POC and PN contents were 0.2 and 0.1 μmol, respectively. Analyses were calibrated against certified reference materials (CRM): IAEA-N1 Ammonium Sulfate (δ^{15}N 0.43‰) and IAEA-305B Ammonium Sulfate (δ^{15}N 375.3‰) for N; and IAEA-CH6 Sucrose (δ^{13}C −10.449‰) and IAEA-309B UL-D-glucose (δ^{13}C 535.3‰) for carbon (C).

2.2.2. Precision and Detection Limit

For every experiment a minimal acceptable increase in isotopic composition of POC and PN at the end of the incubation period [*Montoya et al*., 1996] was defined as being the natural isotopic composition specific to each sample increased by 3 times the uncertainty obtained for isotopic analysis of natural abundance CRM: IAEA-N1 for N, ±0.0003 ^{15}N% (±0.8‰) and IAEA-CH6 for C, ±0.0039 ^{13}C% (±3.5‰). We calculated the minimum uptake rate for each incubation experiment by taking into account all remaining (experiment-specific) terms in equation (1) (e.g., $Æ_{substrate}$, [*Particle*], and Δt). Minimum detectable uptake rates ranged from 0.01 to 0.8 μmol N m^{-3} d^{-1} for N_2 fixation (n = 89 incubations) and from 0.7 to 21.8 μmol C m^{-3} d^{-1} for DIC uptake (n = 89). All measured uptake exceeded their experiment-specific DL.

To obtain the uptake rates uncertainty, we propagated the uncertainty on POC and PN concentration and the standard deviation (SD) of ^{15}N and ^{13}C atom% values of multiple CRM analyses. Precision of the isotopic composition analyses were ±0.0003 ^{15}N% (equivalent to ±0.8‰) for N natural abundance and ±0.0059 ^{15}N% (equivalent to ±16‰) for enriched N CRM. The relative SD (RSD) of the former value was used when calculating the uncertainty for N_2 fixation, since in that case ^{15}N enrichments are relatively close to natural abundance (ranging from 0.366 to 0.413 ^{15}N atom%), while the RSD of enriched CRM was used for C, ±0.0597 ^{13}C% equivalent to ±54‰ (ranging from 1.09 to 2.53 ^{13}C atom%). Depth-integrated rates were calculated by nonuniform gridding trapezoidal integration.

3. Results

3.1. Physical and Biogeochemical Features Along the Transect

The ANT XXIX/1 EUROPA cruise went along the northwest African coast within the Canary Current system then crossed the equatorial upwelling system (EUS) to finally enter a region under influence of the Benguela Current system. All nutrient and uptake rate data are available in supporting information Dataset S1.

Temperature, salinity, dissolved oxygen (O_2), fluorescence [*Rohardt and Wisotzki*, 2013], and nutrient profiles were used to delimit the four biogeographic provinces studied (Figure 2).

The subtropical North Atlantic (STNA, stations 1, 2, 4, and 5) between 20°N and 38°N was the most oligotrophic province, with the lowest surface nutrient concentrations (Figures 2e and 2f) and fluorescence values (Figure 2d) in the upper 100 m. The tropical North Atlantic (TNA, 0°N–20°N, stations 7–10) appeared as the most stratified region as evidenced by strong gradients in the temperature profiles. Sections of nutrient and dissolved O_2 clearly reveal a doming in the TNA due to the presence of the EUS characterized by low oxygen waters and high nutrient advection in subsurface (Figures 2c, 2e and 2f). NO_3^- and PO_4^{3-} were depleted in the upper 25 m, except for PO_4^{3-} at station 7, where a concentration as high as 0.1 μ*M* was observed at the surface while NO_3^- and NH_4^+ were <DL. This results in a local excess of PO_4^{3-} relative to NO_3^- (N/P ≤ 1.0 with N considered as the sum of NO_3^- and NH_4^+), likely due to the proximity of station 7 to the Northwest African upwelling system (see Figure 1). The tropical South Atlantic (TSA, 0°S–15°S, stations 11–14), also

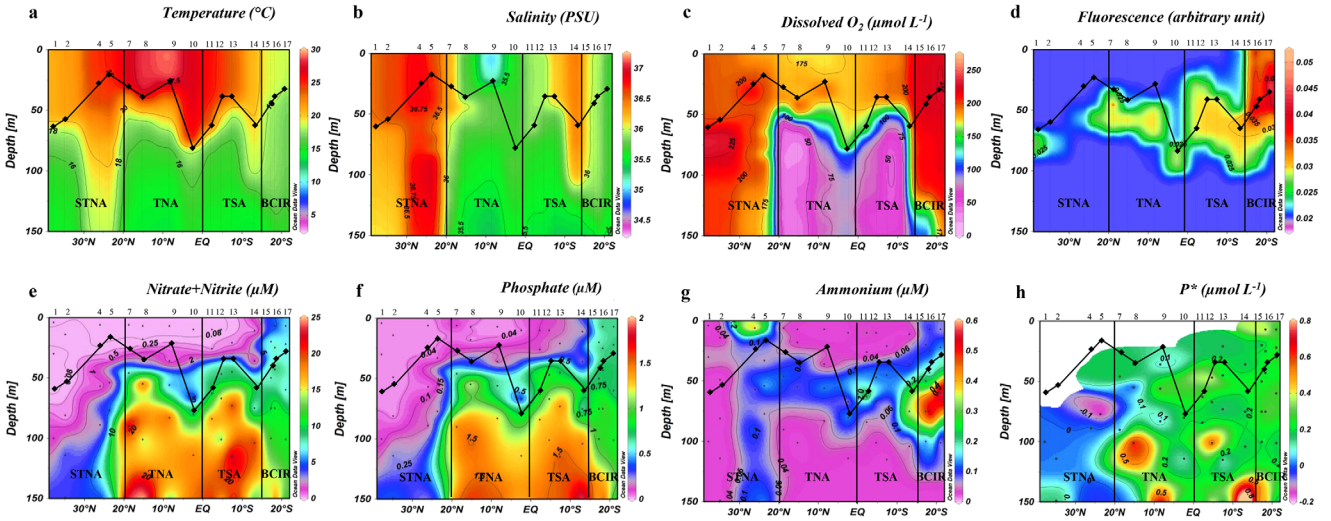

Figure 2. Spatial distribution of (a) temperature, (b) salinity, (c) dissolved O_2, (d) fluorescence, (e) $NO_3^- + NO_2^-$, (f) PO_4^{3-}, (g) NH_4^+, and (h) P* along the ANT XXIX/1 transect. P* = $[PO_4^{3-}] - [NO_3^-]/16$, is based on nutrient data from the present study. Values were omitted when either $NO_3^- + NO_2^-$ or PO_4^{3-} concentrations were below the detection limits (DL), being respectively 80 and 42 nM. Biogeochemical provinces STNA, TNA, TSA, and BCIR as defined in section 3.1. Station positions are indicated on top of the graphs. Mixed layer depths (MLD, black lines connecting diamonds) was estimated using a temperature threshold criterion of 0.2°C relative to the temperature at 10 m [*de Boyer Montégut et al*., 2004].

under influence of the EUS, was characterized similarly by significant subsurface O_2 depletion concomitant with increased nutrient levels reaching shallow waters (~25 m for NO_3^-) and even reaching the surface for PO_4^{3-}. The Benguela Current-influenced region (BCIR, stations 15–17) between 15° and 21°S, had a well-homogenized surface water column (upper 50 m) and was the most nutrient replete. It was likely influenced by the BUS as suggested by the nitrate climatology (November, monthly average NO_3^- concentration for the period 1955–2012, supporting information Figure S1a) revealing a recurrent offshore advection of nutrients from the BUS. These higher nutrient contents sustained higher biomasses in the BCIR as revealed by the high fluorescence (Figure 2d) and the satellite chlorophyll distribution at the time of our study (supporting information Figure S1b) [*Maritorena and Siegel*, 2005]. As for the TNA and TSA provinces, the NH_4^+ profiles in the BCIR showed maximum values in subsurface waters, mimicking the fluorescence profiles. Surface waters of the BCIR were the coolest as a consequence of water upwelling to the surface.

3.2. N_2 Fixation

N_2 fixation activity was detected at all stations and at all investigated PAR levels in the euphotic layer. Results from duplicate incubations (9 out of the 14 stations) were well correlated (regression slope = 1.0, $r^2 = 0.8$, n = 36, $p < 0.001$), thus giving confidence to the results obtained for single replicate incubations at stations 1 and 14–17. Average rates ranged from 0.10 ± 0.02 (avg ± SD) to 12.5 ± 0.4 µmol N m^{-3} d^{-1} (Figures 3a–3d and 4b). The highest N_2 fixation rates were measured in the northern provinces with values ranging from 0.4 to 12.5 µmol N m^{-3} d^{-1} in the TNA (maximum rate at station 7, 50% PAR) and from 0.3 to 4.0 µmol N m^{-3} d^{-1}

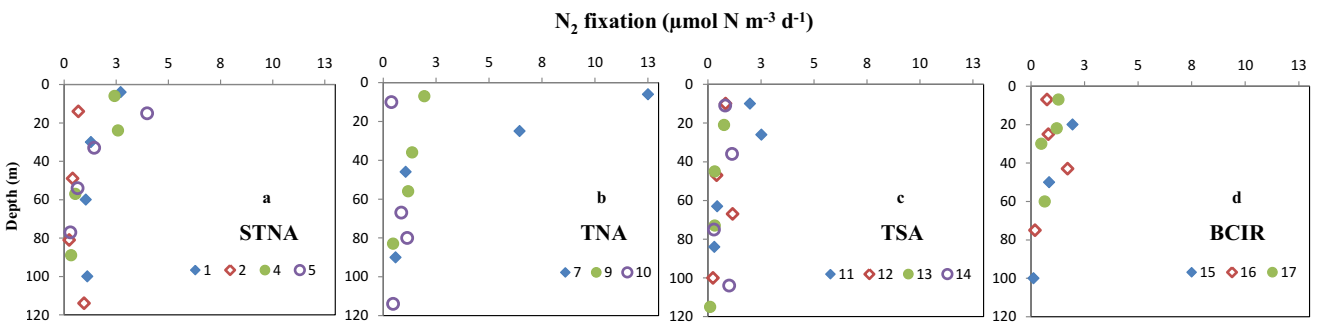

Figure 3. Vertical profiles of averaged N_2 fixation rates (µmol N m^{-3} d^{-1}) within the different biogeochemical provinces studied: (a) STNA, (b) TNA, (c) TSA, and (d) BCIR. Measurements were performed at four depths corresponding to 54%, 15%, 3.5%, and 0.5% of surface irradiance. The median value of relative standard deviation (RSD) considering all duplicate N_2 fixation rates was 34% excluding the 0.5% PAR sample of stations 7 and 13 where one of the replicates was close to the DL (0.02 nmol L^{-1} d^{-1} in both cases).

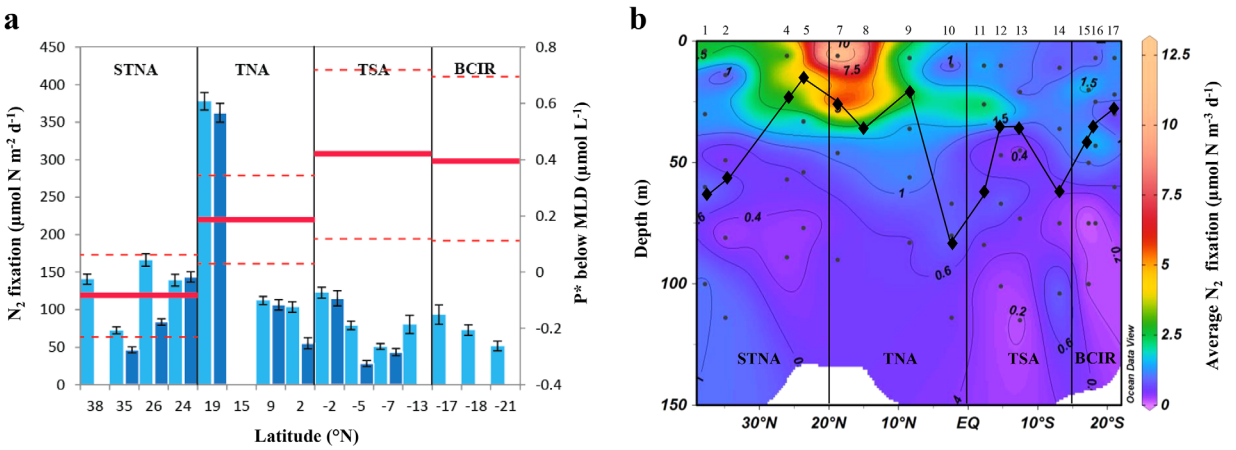

Figure 4. (a) Spatial distribution (±SD) of depth-integrated N_2 fixation rates (replicates A and B in light and dark blue; μmol N m^{-2} d^{-1}); error bars represent the propagated measurement uncertainty of all parameters used to compute volumetric uptake rates. Horizontal red bars indicate province averaged P* (dashed line indicating ± SD) calculated as $[PO_4^{3-}] - [NO_3^-]/16$ (in μmol L^{-1}) between 100 and 700 m depth. (b) ODV section of average N_2 fixation rates (in μmol N m^{-3} d^{-1}); black line represents mixed layer depth.

in the STNA (maximum fixation rate at station 5, 50% PAR). In the southern provinces, we also observed relatively high N_2 fixation rates ranging from 0.1 to 2.5 μmol N m^{-3} d^{-1} in the TSA (maximum rate at station 11, 15% PAR) and from 0.1 to 1.9 μmol N m^{-3} d^{-1} in the BCIR (maximum at station 15, 3.5% PAR). In the TNA and TSA regions low PAR depths coincided with low oxygen waters (dissolved $O_2 \leq 75$ μmol L^{-1}). We did not investigate any possible effect of low oxygen on N_2 fixation, but incubations under anaerobic conditions have been shown to double N_2 fixation rates in the eastern tropical Atlantic [*Staal et al.*, 2007]. However, assuming we underestimated N_2 fixation by twofold at the 0.5% PAR depths (i.e., the only depths that would have been impacted by low oxygen levels in the TNA and TSA sites), the euphotic layer-integrated N_2 fixation rates (for stations 7–13) would increase by only 3–10%. As such, interpretation of our results would not have changed. In general, the vertical distribution of N_2 fixation within all four provinces revealed activity maxima in surface waters (upper 40 m), with values decreasing with depth (Figures 3a–3c and 4b). Euphotic zone-integrated N_2 fixation rates ranged from 47 ± 3 μmol N m^{-2} d^{-1} (station 14, TSA) to 370 ± 9 μmol N m^{-2} d^{-1} (station 7, TNA, Figure 4a). Average euphotic zone-integrated N_2 fixation rates for the four provinces were: 117 ± 39 μmol N m^{-2} d^{-1} (avg ± SD, n = 4, in the STNA), 186 ± 160 μmol N m^{-2} d^{-1} (n = 4, TNA), 75 ± 33 μmol N m^{-2} d^{-1} (n = 4, TSA), and 72 ± 21 μmol N m^{-2} d^{-1} (n = 3, BCIR). A detailed comparison of our results with those from earlier studies is presented in the discussion section 4.1.

3.3. Primary Production (PP)

Duplicate PP measurements were not significantly different (slope = 0.99; $r^2 = 0.89$, n = 34, $p < 0.001$), carbon uptake rates were therefore averaged for further interpretation. Rates of PP ranged from 10 to 2199 μmol C m^{-3} d^{-1} and showed a tendency to increase southward (Figures 5a and 5b). The oligotrophic province (STNA) was the least productive with rates ranging from 27 ± 9 μmol C m^{-3} d^{-1} (avg ± SD, n = 4) to 825 ± 46 μmol C m^{-3} d^{-1} (0.3–9.9 mg C m^{-3} d^{-1}). The most productive province was the BCIR, where PP ranged from 105 ± 19 to 2199 ± 81 μmol C m^{-3} d^{-1} (1.3–26.4 mg C m^{-3} d^{-1}), probably as a result of the influence of the BUS (see above). Indeed, satellite chlorophyll data covering the period of our sampling in the BCIR province reveal an intense phytoplankton activity in the area (supporting information Figure S1b). PP was generally highest in surface waters and decreased gradually with depth. However, at some stations, higher rates were observed in subsurface waters (36–80 m), notably in the EUS: station 10, 80 m (742 ± 40 μmol C m^{-3} d^{-1}); station 13, 45 m (1071 ± 53 μmol C m^{-3} d^{-1}); and station 14, 36 m (756 ± 61 μmol C m^{-3} d^{-1}).

In general, averaged depth-integrated PP for the STNA (24 ± 13 mmol C m^{-2} d^{-1} or 286 ± 158 mg C m^{-2} d^{-1}, avg ± SD, n = 4 stations) and for the whole tropical region between 19°N and 13°S (46 ± 9 mmol C m^{-2} d^{-1}, 556 ± 112 mg C m^{-2} d^{-1}, n = 7) were in the range reported for other Atlantic expeditions, including several meridional transects (Figure 5a and Table 1). However, for the BCIR, average PP rates (74 ± 22 mmol C m^{-2} d^{-1}, 885 ± 259 mg C m^{-2} d^{-1}, n = 3) significantly exceeded the 10–33 mmol C m^{-2} d^{-1}

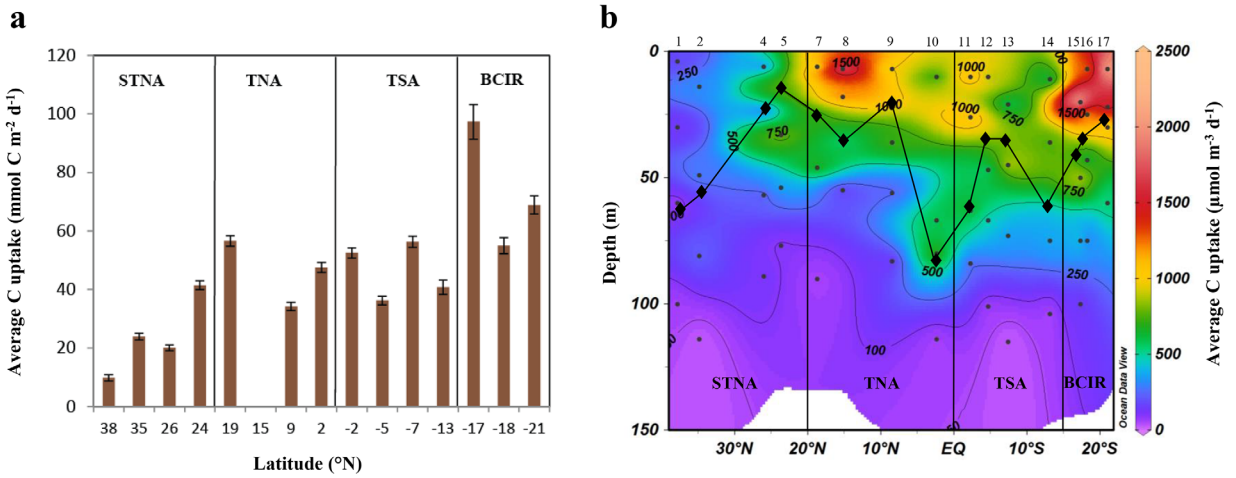

Figure 5. (a) Spatial distribution (±SD) of depth-integrated carbon uptake rates (averaged for duplicate N_2 fixation incubations; mmol C m^{-2} d^{-1}). Error bars represent the propagated measurement uncertainty of all parameters used to compute volumetric uptake rates. (b) ODV section of carbon uptake rates (µmol C m^{-3} d^{-1}); black line represents mixed layer depth.

range reported in earlier Atlantic studies (see Table 1) [*Marañón et al.*, 2000; *Donald et al.*, 2001; *Varela et al.*, 2005; *Pérez et al.*, 2006; *Poulton et al.*, 2006; *Painter et al.*, 2013]. However, the latter studies were conducted mainly at the western boundary of the South Atlantic basin or in the center of the subtropical gyre [*Poulton et al.*, 2006]. The higher PP values we observed for the eastern boundary might therefore be linked to the presence of the BUS.

4. Discussion

The present study investigated oceanic N_2 fixation using the dissolution method [*Mohr et al.*, 2010; *Großkopf et al.*, 2012] over an expanded latitudinal range in the eastern Atlantic Ocean during November 2012. In the following, we discuss (1) the significance of N_2 fixation based on the dissolution method, (2) its contribution to PP, and (3) the potential environmental controlling factors. Finally, (4) we present an updated basin-wide annual estimate of N input to assess the importance of N_2 fixation in the Atlantic marine N cycle.

4.1. Significance of N_2 Fixation in the Different Biogeochemical Provinces

The observed N_2 fixation rates for the North and South Atlantic were similar in magnitude, with no significant difference between the average values for the STNA, TNA, TSA, and BCIR provinces (one-way Anova with and without station 7 maxima, p of 0.28 and 0.27, respectively). Notwithstanding the fact that there is a general slight decreasing trend of N_2 fixation southward, our observations thus highlight that N_2 fixation can be as significant in the eastern South Atlantic as in the eastern North Atlantic.

In the eastern tropical region between 19°N and 13°S (combining TNA and TSA provinces), the observed average N_2 fixation rate of 123 ± 112 µmol N m^{-2} d^{-1} fits within the range of published values for the same period of the year and the same general region and obtained applying either the bubble-addition or the dissolution method (66–194 µmol N m^{-2} d^{-1}, see supporting information Table S1) [*Voss et al.*, 2004; *Moore et al.*, 2009; *Fernández et al.*, 2010; *Turk et al.*, 2011; *Großkopf et al.*, 2012; *Snow et al.*, 2015].

Table 1. Primary Production in the Atlantic Ocean: Comparison With Published Data

	Depth-Integrated Primary Production (mmol C m^{-2} d^{-1})[a]		
	Subtropical North East Atlantic (40°N–25°N)	Tropical East Atlantic (25°N–10°S)	South Atlantic (10°S–40°S)
Range in past studies	6–66	7–54	10–33
Average in present study (±SD)	24 ± 13	46 ± 9	74 ± 22

[a]Average carbon uptake rates in the subtropical North, tropical, and South Atlantic for the present study compared with the range of average measurements reported for the same regions by: *Marañón et al.* [2000], *Donald et al.* [2001], *Joint et al.* [2001], *Varela et al.* [2005], *Pérez et al.* [2006], *Poulton et al.* [2006], and *Painter et al.* [2013].

For the STNA, the average N_2 fixation rate we observed (117 ± 39 μmol N m^{-2} d^{-1}) is in the lower range of those reported elsewhere using the dissolution method (130–162 μmol m^{-2} d^{-1}) [*Großkopf et al*., 2012; *Benavides et al*., 2013a]. Factors such as seasonal variability and different resolutions of vertical sampling schemes (*Großkopf et al*. [2012] and *Benavides et al*. [2013a] performed only surface measurements in the STNA) may account for this relatively small difference. Still, our measurements confirm that values for the eastern STNA obtained via the dissolution method significantly exceed those obtained via the bubble-addition method (from <0.1 to 38 μmol N m^{-2} d^{-1}) [*Moore et al*., 2009; *Fernández et al*., 2010; *Benavides et al*., 2011, 2013b; *Mouriño-Carballido et al*., 2011; *Rijkenberg et al*., 2011; *Turk et al*., 2011; *Fernández et al*., 2013; *Painter et al*., 2013; *Snow et al*., 2015].

In the less explored southeastern Atlantic region (BCIR, south of 10°S), N_2 fixation rates averaged 72 ± 21 μmol N m^{-2} d^{-1}. These rates are close to those reported by *Großkopf et al*. [2012] and *Snow et al*. [2015] for the western South Atlantic (between 10°S and 22°S, 63 to 78 μmol N m^{-2} d^{-1}), but significantly exceed (by a factor 3) the N_2 fixation rates reported by others for the western and eastern South Atlantic (from 3 to 24 μmol N m^{-2} d^{-1} between 10°S and 35°S, excluding data for shelf regions; see supporting information Table S1) [*Moore et al*., 2009; *Fernández et al*., 2010; *Mouriño-Carballido et al*., 2011; *Sohm et al*., 2011b; *Snow et al*., 2015]. We note also that some earlier studies in the eastern South Atlantic did not detect any N_2 fixation using either the acetylene reduction method [*Staal et al*., 2007] or the $^{15}N_2$ dissolution and bubble-addition methods [*Wasmund et al*., 2015].

In the following, we briefly overview the potential factors most likely influencing the difference between the outcomes of the $^{15}N_2$ dissolution and bubble-addition methods.

Several physical and chemical properties inherent to $^{15}N_2$ incubation set up (including incubation duration and agitation, volume of $^{15}N_2$ gas, organic coating at the bubble surface, etc.) have been invoked to explain the discrepancies in N_2 fixation rates between the dissolution and the bubble-addition methods [*Mohr et al*., 2010]. It is therefore difficult to determine which factors mostly set the differences reported between the present study and earlier works using the bubble-addition method. In addition, *Großkopf et al*. [2012] suggested that the diazotrophic community composition could be an additional factor causing these differences between the two methods. They reported greater differences between the dissolution and the bubble-addition (N_2 fixation rates up to 570% higher with the dissolution method) when the community is dominated by smaller diazotrophs (unicellular free or symbiotic cyanobacteria and heterotrophic bacteria) likely because of restricted contact with the $^{15}N_2$ gas bubble during the incubation. When buoyant *Trichodesmium spp*. dominated the community, discrepancies between the methods were indeed less (N_2 fixation rates up to 62% higher with the dissolution method). *Benavides et al*. [2013a] suggested that increased ambient dissolved organic matter (DOM) capable of decelerating the dissolution rate of the $^{15}N_2$ gas bubble, could also play an important role, since differences between the two methods increased with increasing dissolved organic N concentration. Despite lack of evidence, it is worth noting that both previous statements could partly explain the differences observed between our measurements and earlier studies. In fact, for the eastern STNA and BCIR provinces where *Trichodesmium* abundance has been reported to be low to undetectable [*Tyrrell et al*., 2003; *Moore et al*., 2009; *Fernández et al*., 2010; *Mouriño-Carballido et al*., 2011; *Agawin et al*., 2014; *Schlosser et al*., 2014; *Snow et al*., 2015; *Riou et al*., 2016], and DOM concentrations are high due to the proximity of eastern boundary upwelling systems (i.e., northwest Africa and Benguela, respectively) [*Torres-Valdés et al*., 2009; *Letscher et al*., 2013], we find large differences between our results and literature data based on the bubble-addition method. However, we observe smaller discrepancies in the tropical region (TNA + TSA) where *Trichodesmium* has been reported to contribute to at least half of bulk N_2 fixation activity [*Montoya et al*., 2007; *Langlois et al*., 2008; *Foster et al*., 2009; *Goebel et al*., 2010; *Turk et al*., 2011; *Großkopf et al*., 2012; *Ratten et al*., 2015].

4.2. Relative Contribution of N_2 Fixation to Productivity

In the open waters of the Atlantic Ocean, PP was shown to be limited by N availability [*Falkowski*, 1997; *Mills et al*., 2004]. Considering that N_2 fixation is a major source of new N to the euphotic layer, it appears important to investigate its significance for open ocean primary productivity.

We therefore computed the relative contribution of N_2 fixation to PP taking a Redfield ratio of 6.6 for conversion, which matched the median C:N ratio in the natural particles that we collected. While PP was found to increase southward by an order of magnitude (from 10 μmol C m^{-2} d^{-1} at 38°N to 97 μmol C m^{-2} d^{-1}

Table 2. Relative Contribution (%) of N_2 Fixation to Primary Production (PP) and New Production (NP) in the Atlantic Ocean: Comparison With Literature Data

				N_2 Fixation Contribution (%)			
	Reference	Method	Parameter	STNA	TNA	TSA	BCIR
Direct measurements	*Benavides et al.* [2013b]		NP	<1			
	Painter et al. [2013]			3–19[a]			
	Rijkenberg et al. [2011]	$^{15}N_2$ bubble-addition	PP[b]	0.03–5.2			
	Voss et al. [2004]				5.8–12.2		
	Present study	$^{15}N_2$ dissolution method	PP[b]	1.4–9.4	0.8–4.6	0.6–1.1	0.5–0.9
Geochemical estimates	*Capone et al.* [2005]	SPM isotopic mass balance	N demand[c]		36–68		
	Bourbonnais et al. [2009]	NO_3^- isotopic mass balance	Export production	~40			
			Total PP	5			

[a]Range of relative contribution of N_2 fixation to NP considered as new nitrogen uptake in the original publication.
[b]Range of relative contribution of N_2 fixation to PP based on Redfield ratio of 6.6.
[c]Range of relative contribution of N_2 fixation to nitrogen demand (N demand = uptake of $N_2 + NH_4^+ + NO_2^- + NO_3^-$).

at 17°S), the contribution of N_2 fixation as a N source decreased southward but remained quite relevant throughout. On average, N_2 fixation contributed to 5% of PP (n = 4 stations) in the STNA, 2.4% (n = 3) in the TNA, and 0.9% (n = 7) in the combined TSA and BCIR provinces. Station 1 (38°N; STNA) had the highest contribution of N_2 fixation to PP (9%). For the North Atlantic (0°N–38°N), our calculations are similar (see Table 2) to those reported in previous studies based on the bubble-addition method [*Rijkenberg et al*., 2011; *Voss et al*., 2004] as well as on geochemical estimates [*Bourbonnais et al*., 2009].

Furthermore, based on the NO_3^- uptake rates for stations 9–17 (data not presented here; see supporting information data set S1), we computed the relative contribution of N_2 fixation to new production (NP = N_2 fixation/[N_2 fixation + NO_3^- uptake]) assuming that euphotic layer nitrification was negligible. For the region between 8°N and 21°S for which we have NO_3^- uptake results, we observe that N_2 fixation could account for 0.6–2.5% of the NP (n = 8). These results highlight the relevant, albeit small, contribution of N_2 fixation to NP and potential export production even under upwelling-influenced conditions supplying NO_3^- to the surface (i.e., EUS and BUS). Significant N_2 fixation under high ambient NO_3^- concentration has in fact been reported in other studies in the same area [*Voss et al*., 2004; *Sohm et al*., 2011b].

Considering that N_2 fixation rates increased northward (Figure 4) following an intensifying state of oligotrophy (Figure 2), it is reasonable to assume that the contribution of N_2 fixation to NP in the STNA would be larger than in more southward regions. In the same region, *Painter et al*. [2013] reported that N_2 fixation may support up to 19% of NP based on rate measurements (see Table 2).

Geochemical estimates also corroborate a significant contribution of N_2 fixation to export production in the STNA (about 40%) [*Bourbonnais et al*., 2009].

4.3. Environmental Controls on N_2 Fixation Distribution

Diazotrophic activity in the Atlantic Ocean is considered to be limited essentially by Fe [*Moore et al*., 2009] and P availability [*Mills et al*., 2004], and possibly also other trace compounds [*Ho*, 2013; *Jacq et al*., 2014]. Indeed, maximal N_2 fixation rates ($\geq$200 μmol N m^{-2} d^{-1}) in the tropical and subtropical northeast Atlantic have been observed in areas where high Fe input is provided through dry and/or wet deposition of Saharan dust [*Sarthou et al*., 2003; *Moore et al*., 2009; *Fernández et al*., 2010; *Schlosser et al*., 2014; *Snow et al*., 2015]. But, in the South Atlantic, atmospheric Fe inputs are reported to be much less significant than in the north [*Sarthou et al*., 2003; *Moore et al*., 2009; *Fernández et al*., 2010; *Schlosser et al*., 2014; *Snow et al*., 2015]. However, next to Fe, PO_4^{3-} excess relative to NO_3^- is also an important factor that may favor enhanced N_2 fixation [*Deutsch et al*., 2007; *Moore et al*., 2009; *Ratten et al*., 2015]. *Moore et al*. [2009] have indeed suggested that an excess PO_4^{3-} originating from the Southern Ocean (and potentially from the Pacific Ocean) [*Deutsch et al*., 2007] could transit to the North Atlantic advected with Subantarctic Mode Water (SAMW) and Antarctic Intermediate Water (AAIW) and stimulate N_2 fixation activity in the Atlantic Ocean.

In order to explore the potential role of these control factors on our N_2 fixation measurements, we ran a principal component analysis (PCA). This PCA based on Spearman rank correlation investigates the relationship between N_2 fixation rates (we considered volumetric rates in surface waters as well as euphotic layer-integrated rates), phosphorus excess (P*, averaged between 100 and 700 m), and combined dry + wet dust

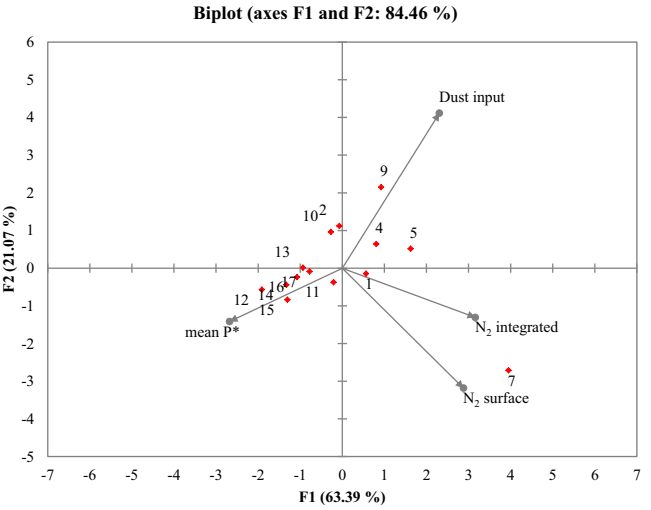

Figure 6. Eucledian distance biplot illustrating the result of PCA based on Spearman rank correlation with surface N_2 fixation rates (μmol Nm^{-3} d^{-1}), euphotic layer-integrated N_2 fixation rates (μmol Nm^{-2} d^{-1}), phosphorus excess (P*, averaged between 100 and 700 m, μmol L^{-1}), and dust input dry + wet deposition derived from satellite data (monthly average values for November 2012; Giovanni online data system, NASA Goddard Earth Sciences Data, and Information Services Center, μg m^{-2} d^{-1}).

input derived from satellite data (we considered the monthly average value for November 2012; Giovanni online data system, NASA Goddard Earth Sciences Data and Information Services Center; see supporting information Table S2). Following Kaiser's rule, two principal components were selected for interpreting the data. These new components explain about 84.5% of the total variance of the system. The Eucledian distance biplot (see Figure 6) shows the factorial design corresponding to the first two axes. The length of a variable vector represents the contribution of the variable to the PCA (i.e., the length of the vector is the square root of the sum of the contributions). In this plot, the position of the stations projected onto a variable vector reflects the relative weights of this variable for each station. This PCA highlights three major points:

(i) The higher N_2 fixation activities in the North Atlantic (stations 1–10), were predominantly related to atmospheric dust deposition; in agreement with observation from earlier works [*Mills et al.*, 2004; *Moore et al.*, 2009; *Fernández et al.*, 2010; *Schlosser et al.*, 2014; *Snow et al.*, 2015]. (ii) Station 7 (19°N), with an N_2 fixation rate between threefold and eightfold higher than at the other sites, behaves differently from the other North Atlantic sites in that next to dust, also P* as well as another, yet undetermined, parameter appeared to influence our measurement. The occurrence of positive P* values we observed in surface waters in the area of station 7 agrees with observations by *Ratten et al.* [2015] and with the 20 m depth P* climatology (October–December; period 1955–2012, Figure 1) [*Garcia et al.*, 2013]. (iii) N_2 fixation in the South Atlantic (stations 11–17) was predominantly related to P*.

Although dust (i.e., iron) and excess phosphate are confirmed as important controlling factors, they operate differently in North and South Atlantic. While dust is most likely a direct controlling factor in the north, in the south a positive P* is profitable to the diazotrophic community, but is itself not sufficient to sustain the relatively high N_2 fixation rates we observe. The absence there of a relationship with dust input implicates the existence of another iron source. According to *Noble et al.* [2012], shelf sediment resuspension within anoxic waters of the BUS, coupled to offshore advection via the Benguela and Angola Currents [*Flohr et al.*, 2014] could represent a major pathway of dissolved Fe input to the eastern South Atlantic. However, Noble et al. also pointed out that the surface concentration of iron originating from coastal sediments, rapidly decreased with distance from the shelf likely due to oxidation and scavenging. Thus, the offshore input of iron would be spatially limited. Noble et al. reported nevertheless significant iron concentration up to 1.0 n*M* in subsurface waters (200–400 m) of the eastern South Atlantic as far offshore as the prime meridian covering the area of the South Atlantic sites studied here (see Figure 1). As such, during active upwelling in the Benguela region waters advected offshore could carry both iron and excess phosphorus to sustain N_2 fixation activity. Temperature, salinity, and nutrients sections from stations we sampled in the BCIR province (station 15–17, located between 17°S and 21°S and 3°E and 6°E) suggest these locations were characterized by a well-homogenized nitrate and phosphate replete surface layer. In addition, nitrate climatology (November, monthly average NO_3^- concentration for the period 1955–2012, supporting information Figure S1a) along with enhanced chlorophyll concentration recorded by satellite data at the time of our cruise (supporting information Figure S1b) in the eastern South Atlantic sampled region, indicate a plausible influence of the upwelling in the area of station 15–17.

Our field measurements of N_2 fixation activity and circumstantial evidence from satellite data and nutrient climatology therefore seem to point toward the critical role of atmospheric dust deposition and eastern

Table 3. Estimates of N Inputs to the Open Atlantic Ocean

	Reference	Method	Ocean Area (10^6 km^2)	N Input ($\pm$SE; Tg N yr^{-1})	Domain
Direct measurements	*Capone et al.* [2005]	Scaled in situ measurements of *Trichodesmium* N_2 fixation	18–28	22–34	North Atlantic
	Großkopf et al. [2012]	Scaled own N_2 fixation measurements		24 ± 1	25°N–45°S
	Luo et al. [2012]	Compilation of published	36	32 ± 7.4	0°N–55°N
		oceanic N_2 fixation measurements	27	2 ± 0.6	0°S–40°S
	Present study	Scaled present-study N_2 fixation measurements	42	25.1 ± 5.6	38°N–21°S
	Compiled N_2 fixation data from the Atlantic Ocean	Scaled N_2 fixation of studies using the	19	3.1 ± 1.5	20°N–50°N
		acetylene reduction assay, the $^{15}N_2$	21	19.5 ± 10	20°N–10°S
		bubble-addition and dissolution	28	5.0 ± 2.0	10°S–45°S
		methods including data from the present study	68	27.6 ± 10	50°N–45°S
Geochemical estimates	*Gruber and Sarmiento* [1997]	Thermocline $N^* = ([NO_3^-] - 16 \times [PO_4^{3-}] + 2.90) \times 0.87$	28	28	10°N–50°N
	Singh et al. [2013]	Subsurface water column $N^* = [NO_3^-] - 14.63 \times [PO_4^{3-}]$	28	17	0°N–50°N
	Deutsch et al. [2007]	Surface waters $P^* = [PO_4^{3-}] - [NO_3^-]/16$	63	20	65°N–40°S
	Knapp et al. [2008]	Water column nitrate isotopic composition		21–34	45°N–45°S
	Lee et al. [2002]	Carbon inventory assuming a C:N ratio of 7:1 for biomass	46	28	40°N–40°S
	Moore et al. [2009]	Water column $N^* = [NO_3^-] - 16 \times [PO_4^{3-}]$		15–21	36°N–30°S

boundary upwelling systems in sustaining offshore N_2 fixation activity. In the North Atlantic, the input of Fe-rich atmospheric dust, and also regionally the advection of P-rich waters (case of station 7), likely triggered the observed high N_2 fixation rates. In the South Atlantic, positive P* signatures combined with a potential input of dissolved Fe and other trace elements from the BUS likely triggered the relatively high N_2 fixation rates observed there.

4.4. Revisiting the Annual N_2 Fixation Rates

In this section, we discuss basin-wide estimates of annual N input to the ocean resulting from diazotrophic activity. For the Atlantic Ocean region bounded by 38°N and 21°S, we estimated an annual N_2 fixation rate of 25.1 ± 5.6 Tg N yr^{-1} based on our measurements. However, these calculations cover limited spatial and temporal scales, and so we attempted to integrate our measured values in a broader data set to come up with a more representative figure for diazotroph-sustained N input into the Atlantic.

We combined our results with published Atlantic open ocean data (including for example earlier works such as *Orcutt et al.*, 2001; *Krupke et al.*, 2013; *Subramaniam et al.*, 2013; see supporting information Table S1). Based on the available measurements, we could cover the northern region between 20°N and 50°N, the tropical region from 20°N to 10°S and the southern basin between 10°S–45°S (see supporting information Table S1). We considered the tropical basin to extend southward down to 10°S, corresponding to the southernmost migration boundary of the Intertropical Convergence Zone (ITCZ) [*Chiang et al.*, 2002]. Since the ITCZ is considered to act as a barrier to Saharan dust input to the South Atlantic [*Schlosser et al.*, 2014], the tropical region which is the most impacted by dust input could thereby be considered as a single system. We computed average N inputs weighted by the number of sites visited during the different studies, for each of the three latitudinal regions to minimize the influence of intensive sampling in the northwestern tropical hot spot area. Since observations close to margins and shelves, which reveal relatively high rates of N_2 fixation, are still scarce, we chose to exclude data from those areas (see supporting information Table S1). This concerns data from the Gulf of Mexico [*Holl et al.*, 2007], the English Channel [*Rees et al.*, 2009], the BUS [*Sohm et al.*, 2011b] (but for the latter, data for stations outside the upwelling area were still considered), the North American coastal waters [*Mulholland et al.*, 2012], and the South American shelf-influenced region [*Snow et al.*, 2015] (but data collected east of 40°W during the JC32 cruise were considered). Nonetheless a proper assessment of the significance of margins and shelves at the global scale, clearly calls for more measurements in those systems.

We calculated an annual N input for the whole Atlantic Ocean of 27.6 ± 10.4 Tg N yr^{-1} ($\pm$standard error, SE, see Table 3), with the N input in the tropical region (19.5 ± 10.1 Tg N yr^{-1}; 20°N–10°S) exceeding by about sixfold and threefold that in the northern region (3.1 ± 1.5 Tg N yr^{-1}; 20°N–50°N) and the southern basin (5.0 ± 2.0 Tg N yr^{-1}; 10°S–45°S), respectively.

Our value for the global Atlantic is in the range of the 34 Tg N yr^{-1} reported by *Luo et al.* [2012] for the region bounded by 55°N and 40°S, although it is slightly lower since we did not included shelf and margin measurements as they did (which would increase our estimate to a value of 33.2 ± 11.2 Tg N yr^{-1}), and since we also considered more recent studies in our computation. In line with this, while the contribution of the northern basin is decreased, our estimate for the South Atlantic appears to be twofold larger (2 Tg N yr^{-1}; 0°S–40°S) than in the compilation by [*Luo et al.*, 2012], likely owing to the inclusion of recent data [*Großkopf et al.*, 2012; *Snow et al.*, 2015, and present study]. The latter data are in fact up to an order of magnitude larger than previous results for the South Atlantic considered by Luo et al. (see supporting information Table S1). We also find that our estimates are in the range of geochemically estimated N input values for the North Atlantic (between 17 and 28 Tg N yr^{-1}) [*Gruber and Sarmiento*, 1997; *Singh et al.*, 2013] and the whole Atlantic Ocean (between 15 and 34 Tg N yr^{-1}, see Table 3) [*Lee et al.*, 2002; *Deutsch et al.*, 2007; *Knapp et al.*, 2008; *Moore et al.*, 2009].

These findings point toward a greater role of the South Atlantic in the global N cycle than previously thought, and highlight the urgent need for more N_2 fixation data in the South Atlantic in order to better constrain annual N input fluxes. Finally, the obtained N input values for the South Atlantic (5 Tg N yr^{-1}) suggest that N_2 fixation might balance the loss of fixed N through the combined effect of anammox (1.4 Tg N yr^{-1}) [*Kuypers et al.*, 2005] and denitrification ($\sim$2.5 Tg N yr^{-1}) [*Nagel et al.*, 2013] within the oxygen minimum zone of the BUS. Despite this near balance, South Atlantic surface waters still exhibit a significant P*, which then is likely inherited from the Indo-Pacific and advected with thermocline/intermediate waters formed in the Southern Ocean, as proposed by *Moore et al.* [2009].

5. Conclusions

The present work adds to the existing data set on community dinitrogen (N_2) fixation measurements in the Atlantic Ocean. Results highlight the fact that the nitrogen (N) input in the eastern South Atlantic and the role of this region in the global basin N cycle have been underestimated and should be reconsidered. We support the hypothesis that eastern boundary upwelling (northwest Africa and Benguela) in the Atlantic Ocean fuel offshore regions with excess phosphorus (P) and potentially trace elements and thus contribute to sustaining significant N_2 fixation activity. N_2 fixation was shown to fuel up to 9% of primary production (PP) in the oligotrophic subtropical North Atlantic (STNA, 20°N–38°N) while in the nutrient replete Benguela Current-influenced region (BCIR, 15°S–21°S) N_2 fixation contributed to about 1% and 2% of PP and new production (NP), respectively. Annual basin-scale N_2 fixation rates obtained by combining our data with data from previous studies are in agreement with the overall assessment by *Luo et al.* [2012]. However, our calculations also highlight a larger contribution by the South Atlantic diazotrophic activity. Although we observed a significant consistency in our replicate experiments, data collected in the 13°S–21°S latitudinal range was not duplicated; there is thus a need to further investigate N_2 fixation spatial and temporal variabilities in the eastern South Atlantic to confirm our findings. Large discrepancies existing between published data obtained with different methods also stress the need for a standardized methodological approach for future studies. Finally, the contribution from margin and shelf areas, potentially influenced by large riverine input (e.g., Amazon and Congo) needs more detailed investigations as these areas might harbor a great deal of diazotrophic activity, which presently is not well accounted for in annual basin-wide estimates.

Acknowledgments

We thank the Captain and the crew of R/V Polarstern for their skillful support and the Alfred Wegener Institute for Polar and Marine Research, Bremerhaven. The enthusiasm and help of graduate students L. Brunelli, C. Gil-Fernandez, M. Rembauville, D. Ribicic and, T. Schwenke during the Europa cruise greatly contributed to the outcome of this work. We thank D. Verstraeten and J. Aristegui for their assistance with experimental work. Nutrients and uptake rates data for this paper are available in supporting information data set S1. This work was financed by the Flanders Research Foundation (FWO contract G071512N) and the Vrije Universiteit Brussel, R&D, Strategic Research Plan "Tracers of Past & Present Global Changes." This work is also a contribution to the Labex OT-Med (ANR-11-LABEX-0061, www.otmed.fr) funded by the Investissements d'Avenir, French Government project of the French National Research Agency (ANR, www.agence-nationale-recherche.fr) through the A*Midex project (ANR-11-IDEX-0001-02), funding V. Riou during the preparation of the manuscript.

References

Agawin, N. S. R., M. Benavides, A. Busquets, P. Ferriol, L. J. Stal, and J. Arístegui (2014), Dominance of unicellular cyanobacteria in the diazotrophic community in the Atlantic Ocean, *Limnol. Oceanogr.*, *59*(2), 623–637, doi:10.4319/lo.2014.59.2.0623.

Benavides, M., N. Agawin, J. Arístegui, P. Ferriol, and L. Stal (2011), Nitrogen fixation by Trichodesmium and small diazotrophs in the subtropical northeast Atlantic, *Aquat. Microb. Ecol.*, *65*(1), 43–53, doi:10.3354/ame01534.

Benavides, M., D. A. Bronk, N. S. R. Agawin, M. D. Pérez-Hernández, A. Hernández-Guerra, and J. Arístegui (2013a), Longitudinal variability of size-fractionated N_2 fixation and DON release rates along 24.5°N in the subtropical North Atlantic, *J. Geophys. Res. Oceans*, *118*, 3406–3415, doi:10.1002/jgrc.20253.

Benavides, M., J. Arístegui, N. S. R. Agawin, X. A. Álvarez-Salgado, M. Álvarez, and C. Troupin (2013b), Low contribution of N_2 fixation to new production and excess nitrogen in the subtropical northeast Atlantic margin, *Deep Sea Res., Part I*, *81*, 36–48, doi:10.1016/j.dsr.2013.07.004.

Berman-Frank, I., J. T. Cullen, Y. Shaked, R. M. Sherrell, and P. G. Falkowski (2001), Iron availability, cellular iron quotas, and nitrogen fixation in Trichodesmium, *Limnol. Oceanogr.*, *46*(6), 1249–1260, doi:10.4319/lo.2001.46.6.1249.

Bourbonnais, A., M. F. Lehmann, J. J. Waniek, and D. E. Schulz-Bull (2009), Nitrate isotope anomalies reflect N_2 fixation in the Azores Front region (subtropical NE Atlantic), *J. Geophys. Res.*, *114*, C03003, doi:10.1029/2007JC004617.

Braman, R. S., and S. A. Hendrix (1989), Nanogram nitrite and nitrate determination in environmental and biological materials by vanadium (III) reduction with chemiluminescence detection, *Anal. Chem.*, *61*(24), 2715–2718, doi:10.1021/ac00199a007.

Capone, D. G., J. A. Burns, J. P. Montoya, A. Subramaniam, C. Mahaffey, T. Gunderson, Michaels, A. F., and E. J. Carpenter (2005), Nitrogen fixation by Trichodesmium spp.: An important source of new nitrogen to the tropical and subtropical North Atlantic Ocean, *Global Biogeochem. Cycles*, *19*, GB2024, doi:10.1029/2004GB002331.

Charria, G., I. Dadou, J. Llido, M. Drevillon, and V. Garcon (2008), Importance of dissolved organic nitrogen in the north Atlantic Ocean in sustaining primary production: A 3-D modelling approach, *Biogeosciences*, *5*(5), 1437–1455, doi:10.5194/bg-5-1437-2008.

Chiang, J. C. H., Y. Kushnir, and A. Giannini (2002), Deconstructing Atlantic Intertropical Convergence Zone variability: Influence of the local cross-equatorial sea surface temperature gradient and remote forcing from the eastern equatorial Pacific, *J. Geophys. Res.*, *107*(D1), 4004, doi:10.1029/2000JD000307.

Codispoti, L. A. (2007), An oceanic fixed nitrogen sink exceeding 400 Tg N a-1 vs the concept of homeostasis in the fixed-nitrogen inventory, *Biogeosciences*, *4*, 233–253, doi:10.5194/bgd-3-1203-2006.

Codispoti, L. A., J. A. Brandes, J. P. Christensen, A. H. Devol, S. W. A. Naqvi, H. W. Paerl, and T. Yoshinari (2001), The oceanic fixed nitrogen and nitrous oxide budgets: Moving targets as we enter the anthropocene?, *Sci. Mar.*, *65*(2), 85–105, doi:10.3989/scimar.2001.65s285.

Dabundo, R., M. F. Lehmann, L. Treibergs, C. R. Tobias, M. A. Altabet, P. H. Moisander, and J. Granger (2014), The contamination of commercial $15N_2$ gas stocks with 15N-labeled nitrate and ammonium and consequences for nitrogen fixation measurements, *PloS One*, *9*(10), e110335, doi:10.1371/journal.pone.0110335.

De Boyer Montégut, C., G. Madec, A. S. Fischer, A. Lazar, and D. Iudicone (2004), Mixed layer depth over the global ocean: An examination of profile data and a profile-based climatology, *J. Geophys. Res.*, *109*, C12003, doi:10.1029/2004JC002378.

Deutsch, C., J. L. D. S. M. Sigman, N. Gruber, and J. P. Dunne (2007), Spatial coupling of nitrogen inputs and losses in the ocean, *Nature*, *445*(7124), 163–167, doi:10.1038/nature05392.

Donald, K. M., I. Joint, A. P. Rees, E. M. S. Woodward, and G. Savidge (2001), Uptake of carbon, nitrogen and phosphorus by phytoplankton along the 20°W meridian in the NE Atlantic between 57.5°N and 37°N, *Deep Sea Res., Part II*, *48*(4-5), 873–897, doi:10.1016/S0967-0645(00)00102-8.

Dugdale, R. C., and J. J. Goering (1967), Uptake of new and regenerated forms of nitrogen in primary productivity, *Limnol. Oceanogr.*, *12*(2), 196–206, doi:10.4319/lo.1967.12.2.0196.

Dugdale, R. C., and F. P. Wilkerson (1986), The use of 15N to measure nitrogen uptake in eutrophic oceans: Experimental considerations, *Limnol. Oceanogr.*, *31*(4), 673–689, doi:10.4319/lo.1986.31.4.0673.

Falcón, L. I., E. J. Carpenter, F. Cipriano, B. Bergman, and D. G. Capone (2004), N_2 fixation by unicellular bacterioplankton from the Atlantic and Pacific Oceans: Phylogeny and in situ rates, *Appl. Environ. Microbiol.*, *70*(2), 765–770, doi:10.1128/AEM.70.2.765.

Falkowski, P. G. (1997), Evolution of the nitrogen cycle and its influence on the biological sequestration of CO_2 in the ocean, *Nature*, *387*(6630), 272–275, doi:10.1038/387272a0.

Fernández, A., B. Mouriño-Carballido, A. Bode, M. Varela, and E. Marañón (2010), Latitudinal distribution of Trichodesmium spp. and N_2 fixation in the Atlantic Ocean, *Biogeosci. Discuss.*, *7*(2), 2195–2225, doi:10.5194/bgd-7-2195-2010.

Fernández, A., R. Graña, B. Mouriño-Carballido, A. Bode, M. Varela, J. F. Domínguez-Yanes, J. Escánez, D. Armas, and E. Marañón (2013), Community N_2 fixation and Trichodesmium spp. abundance along longitudinal gradients in the eastern subtropical North Atlantic, *ICES J. Mar. Sci.*, *70*(1), 223–231, doi:10.1093/icesjms/fst176.

Fitzsimmons, J. N., R. Zhang, and E. A. Boyle (2013), Dissolved iron in the tropical North Atlantic Ocean, *Mar. Chem.*, *154*, 87–99, doi:10.1016/j.marchem.2013.05.009.

Flohr, A., A. K. Van Der Plas, K. C. Emeis, V. Mohrholz, and T. Rixen (2014), Spatio-temporal patterns of C : N : P ratios in the northern Benguela upwelling system, *Biogeosciences*, *11*(3), 885–897, doi:10.5194/bg-11-885-2014.

Foster, R. A., A. Subramaniam, and J. P. Zehr (2009), Distribution and activity of diazotrophs in the Eastern Equatorial Atlantic, *Environ. Microbiol.*, *11*(4), 741–50, doi:10.1111/j.1462-2920.2008.01796.x.

Fry, B. (2003), Steady state models of stable isotopic distributions, *Isotopes Environ. Health Stud.*, *39*(3), 219–232, doi:10.1080/1025601031000108651.

Garcia, H. E., R. A. Locarnini, T. P. Boyer, J. I. Antonov, O. K. Baranova, M. M. Zweng, J. R. Reagan, and D. R. Johnson (2013), *World Ocean Atlas 2013. Vol. 4. Dissolved Inorganic Nutrients (Phosphate, Nitrate, Silicate), NOAA Atlas NESDIS 76*, edited by S. Levitus and A. Mishonov, 25 pp., Silver Spring, Md.

Goebel, N. L., K. A. Turk, K. M. Achilles, R. Paerl, I. Hewson, A. E. Morrison, J. P. Montoya, C. A. Edwards, and J. P. Zehr (2010), Abundance and distribution of major groups of diazotrophic cyanobacteria and their potential contribution to N_2 fixation in the tropical Atlantic Ocean, *Environ. Microbiol.*, *12*(12), 3272–3289, doi:10.1111/j.1462-2920.2010.02303.x.

Gordon, H. R. (1997), Atmospheric correction of ocean color imagery in the Earth Observing System era, *J. Geophys. Res.*, *102*(D14), 17,081–17,106.

Granger, J., and D. M. Sigman (2009), Removal of nitrite with sulfamic acid for nitrate N and O isotope analysis with the denitrifier method, *Rapid Commun. Mass Spectrom.*, *23*, 3753–3762, doi:10.1002/rcm.4307.

Grasshoff, K., M. Ehrhardt, and K. Kremling (1983), *Methods of Seawater Analysis*, 2nd, revised and extended edition, Verlag Chemie GmbH, D-6940 Weinheim, Germany.

Großkopf, T., W. Mohr, T. Baustian, H. Schunck, D. Gill, M. M. M. Kuypers, G. Lavik, R. A. Schmitz, D. W. R. Wallace, and J. LaRoche (2012), Doubling of marine dinitrogen-fixation rates based on direct measurements, *Nature*, *488*(7411), 361–364, doi:10.1038/nature11338.

Gruber, N. (2008), The marine nitrogen cycle: Overview and challenges, in *Nitrogen in the Marine Environment*, pp. 1–50, Elsivier Inc., Amsterdam, Netherlands, doi:10.1016/B978-0-12-372522-6.00001-3.

Gruber, N., and J. L. Sarmiento (1997), Global patterns of marine nitrogen fixation and denitrification, *Global Biogeochem. Cycles*, *11*(2), 235–266, doi:10.1029/97GB00077.

Gruber, N., and J. L. Sarmiento (2002), Large scale biochemical/physical interactionsin elemental cycles, in *The Sea: Biological-Physical Interactions in the Oceans*, vol. 12, pp. 337–399, John Wiley and Sons, Inc., New York.

Hama, T., T. Miyazaki, Y. Ogawa, T. Iwakuma, M. Takahashi, A. Otsuki, and S. Ichimura (1983), Measurement of photosynthetic production of a marine phytoplankton population, *Mar. Biol.*, *73*, 31–36.

Ho, T.-Y. (2013), Nickel limitation of nitrogen fixation in Trichodesmium, *Limnol. Oceanogr.*, *58*(1), 112–120, doi:10.4319/lo.2013.58.1.0112.

Holl, C. M., T. D. Clayton, and J. P. Montoya (2007), Trichodesmium in the western Gulf of Mexico: $15N_2$-fixation and natural abundance stable isotope evidence, *Limnol. Oceanogr.*, *52*(5), 2249–2259.

Holmes, R. M., A. Aminot, R. Kérouel, B. A. Hooker, and B. J. Peterson (1999), A simple and precise method for measuring ammonium in marine and freshwater ecosystems, *Can. J. Fish. Aquat. Sci.*, *56*(10), 1801–1808, doi:10.1139/f99-128.

Jacq, V., C. Ridame, S. L'Helguen, F. Kaczmar, and A. Saliot (2014), Response of the unicellular diazotrophic cyanobacterium Crocosphaera watsonii to iron limitation, *PloS One*, *9*(1), e86749, doi:10.1371/journal.pone.0086749.

Joint, I., A. P. Rees, and E. M. S. Woodward (2001), Primary production and nutrient assimilation in the Iberian upwelling in August 1998, *Progress in Oceanography*, *51*(2–4), 303–320, doi:10.1016/S0079-6611(01)00072-6.

Klawonn, I., G. Lavik, P. Böning, H. K. Marchant, J. Dekaezemacker, W. Mohr, and H. Ploug (2015), Simple approach for the preparation of 15 − 15N_2-enriched water for nitrogen fixation assessments: Evaluation, application and recommendations, *Frontiers Microbiol.*, *6*(August), 1–11, doi:10.3389/fmicb.2015.00769.

Knapp, A. N., DiP. J. Fiore, C. Deutsch, D. M. Sigman, and F. Lipschultz (2008), Nitrate isotopic composition between Bermuda and Puerto Rico: Implications for N_2 fixation in the Atlantic Ocean, *Global Biogeochem. Cycles*, *22*, GB3014, doi:10.1029/2007GB003107.

Krupke, A., N. Musat, J. LaRoche, W. Mohr, B. M. Fuchs, R. I. Amann, M. M. M. Kuypers, and R. A. Foster (2013), In situ identification and N_2 and C fixation rates of uncultivated cyanobacteria populations, *Syst. Appl. Microbiol.*, *36*(4), 259–271, doi:10.1016/j.syapm.2013.02.002.

Kuypers, M. M. M., G. Lavik, D. Woebken, M. Schmid, B. M. Fuchs, R. Amann, B. B. Jørgensen, and M. S. M. Jetten (2005), Massive nitrogen loss from the Benguela upwelling system through anaerobic ammonium oxidation, *Proc. Natl. Acad. Sci. U. S. A.*, *102*(18), 6478–83, doi:10.1073/pnas.0502088102.

Lagerström, M. E., M. P. Field, M. Séguret, L. Fischer, S. Hann, and R. M. Sherrell (2013), Automated on-line flow-injection ICP-MS determination of trace metals (Mn, Fe, Co, Ni, Cu and Zn) in open ocean seawater: Application to the GEOTRACES program, *Mar. Chem.*, *155*, 71–80, doi:10.1016/j.marchem.2013.06.001.

Langlois, R., M. Mills, C. Ridame, P. Croot, and J. LaRoche (2012), Diazotrophic bacteria respond to Saharan dust additions, *Mar. Ecol. Prog. Ser.*, *470*, 1–14, doi:10.3354/meps10109.

Langlois, R. J., D. Hümmer, and J. LaRoche (2008), Abundances and distributions of the dominant nifH phylotypes in the Northern Atlantic Ocean, *Appl. Environ. Microbiol.*, *74*(6), 1922–1931, doi:10.1128/AEM.01720-07.

Lee, K., D. M. Karl, R. Wanninkhof, and J.-Z. Zhang (2002), Global estimates of net carbon production in the nitrate-depleted tropical and subtropical oceans, *Geophys. Res. Lett.*, *29*(19), 1907, doi:10.1029/2001GL014198.

Letscher, R. T., D. A. Hansell, C. A. Carlson, R. Lumpkin, and A. N. Knapp (2013), Dissolved organic nitrogen in the global surface ocean: Distribution and fate, *Global Biogeochem. Cycles*, *27*, 141–153, doi:10.1029/2012GB004449.

Luo, Y.-W., et al. (2012), Database of diazotrophs in global ocean: Abundance, biomass and nitrogen fixation rates, *Earth Syst. Sci. Data*, *4*(1), 47–73, doi:10.5194/essd-4-47-2012.

Mahaffey, C., R. G. Williams, and G. A. Wolff (2004), Physical supply of nitrogen to phytoplankton in the Atlantic Ocean, *Global Biogeochem. Cycles*, *18*, 1–13, doi:10.1029/2003GB002129.

Mahaffey, C., A. F. Michaels, and D. G. Capone (2005), The conundrum of marine N_2 fixation, *Am. J. Sci.*, *305*, 546–595, doi:10.2475/ajs.305.6-8.546.

Marañón, E., P. M. Holligan, M. Varela, B. Mouriño, and A. J. Bale (2000), Basin-scale variability of phytoplankton biomass, production and growth in the Atlantic Ocean, *Deep Sea Res., Part I*, *47*, 825–857, doi:10.1016/S0967-0637(99)00087-4.

Maritorena, S., and D. A. Siegel (2005), Consistent merging of satellite ocean colour data sets using a bio-optical model, *Remote Sens. Environ.*, *94*(4), 429–440.

Mawji, E., et al. (2015), The GEOTRACES intermediate data product 2014, *Mar. Chem.*, *177*, 1–8, doi:10.1016/j.marchem.2015.04.005.

McIlvin, M. R., and M. A. Altabet (2005), Chemical conversion of nitrate and nitrite to nitrous oxide for nitrogen and oxygen isotopic analysis in freshwater and seawater, *Anal. Chem.*, *77*(17), 5589–5595, doi:10.1021/ac050528s.

Mills, M. M., C. Ridame, M. Davey, J. La Roche, and R. J. Geider (2004), Iron and phosphorus co-limit nitrogen fixation in the eastern tropical North Atlantic, *Nature*, *429*(6989), 292–294, doi:10.1038/nature03632.

Miyajima, T., Y. Yamada, Y. T. Hanaba, K. Yoshii, K. Koitabashi, and E. Wada (1995), Determining the stable isotope ratio of total dissolved inorganic carbon in lake water by GC/C/IRMS, *Limnol. Oceanogr.*, *40*(5), 994–1000.

Mohr, W., T. Großkopf, D. W. R. Wallace, and J. LaRoche (2010), Methodological underestimation of oceanic nitrogen fixation rates, *PLoS ONE*, *5*(9), 1–7, doi:10.1371/journal.pone.0012583.

Montoya, J. P., M. Voss, P. Kahler, and D. G. Capone (1996), A Simple, High-Precision, High-Sensitivity Tracer Assay for N2 Fixation, *Appl. Environ. Microbiol.*, *62*(3), 986–993.

Montoya, J. P., M. Voss, and D. G. Capone (2007), Spatial variation in N_2-fixation rate and diazotroph activity in the Tropical Atlantic, *Biogeosciences*, *4*(3), 369–376, doi:10.5194/bg-4-369-2007.

Moore, C. M., et al. (2009), Large-scale distribution of Atlantic nitrogen fixation controlled by iron availability, *Nat. Geosci.*, *2*(12), 867–871, doi:10.1038/ngeo667.

Mouriño-Carballido, B., R. Graña, A. Fernàndez, A. Bode, M. Varela, J. F. Domínguez, M. J. Follows, and E. Marañón (2011), Importance of N_2 fixation vs. nitrate eddy diffusion along a latitudinal transect in the Atlantic Ocean, *Limnol. Oceanogr.*, *56*(3), 999–1007, doi:10.4319/lo.2011.56.3.0999.

Mulholland, M. R., P. W. Bernhardt, J. L. Blanco-Garcia, A. Mannino, K. Hyde, E. Mondragon, K. Turk, P. H. Moisander, and J. P. Zehr (2012), Rates of dinitrogen fixation and the abundance of diazotrophs in North American coastal waters between Cape Hatteras and Georges Bank, *Limnol. Oceanogr.*, *57*(4), 1067–1083, doi:10.4319/lo.2012.57.4.1067.

Nagel, B., K.-C. Emeis, A. Flohr, T. Rixen, T. Schlarbaum, V. Mohrholz, and A. van der Plas (2013), N-cycling and balancing of the N-deficit generated in the oxygen minimum zone over the Namibian shelf-An isotope-based approach, *J. Geophys. Res. Biogeosci.*, *118*, 361–371, doi:10.1002/jgrg.20040.

Noble, A. E., C. H. Lamborg, D. C. Ohnemus, P. J. Lam, T. J. Goepfert, C. I. Measures, C. H. Frame, K. L. Casciotti, G. R. DiTullio, J. Jennings, and M. A. Saito (2012), Basin-scale inputs of cobalt, iron, and manganese from the Benguela-Angola front to the South Atlantic Ocean, *Limnol. Oceanogr.*, *57*(4), 989–1010, doi:10.4319/lo.2012.57.4.0989.

Orcutt, K. M., F. Lipschultz, K. Gundersen, R. Arimoto, A. F. Michaels, A. H. Knap, and J. R. Gallon (2001), A seasonal study of the significance of N_2 fixation by Trichodesmium spp. at the Bermuda Atlantic Time-series Study (BATS) site, *Deep Sea Res., Part II*, *48*(8-9), 1583–1608, doi:10.1016/S0967-0645(00)00157-0.

Paerl, H. W., K. M. Crocker, and L. E. Prufert (1987), Limitation of N_2 fixation in coastal marine waters: Relative importance of molybdenum, iron, phosphorus, and organic matter availability, *Limnol. Oceanogr.*, *32*(May), 525–536, doi:10.4319/lo.1987.32.3.0525.

Painter, S. C., M. D. Patey, A. Forryan, and S. Torres-Valdes (2013), Evaluating the balance between vertical diffusive nitrate supply and nitrogen fixation with reference to nitrate uptake in the eastern subtropical North Atlantic Ocean, *J. Geophys. Res. Oceans*, *118*, 5732–5749, doi:10.1002/jgrc.20416.

Pérez, V., E. Fernández, E. Marañón, X. A. G. Morán, and M. V. Zubkov (2006), Vertical distribution of phytoplankton biomass, production and growth in the Atlantic subtropical gyres, *Deep Sea Res., Part I*, *53*(10), 1616–1634, doi:10.1016/j.dsr.2006.07.008.

Peterson, R. G., and L. Stramma (1991), Upper-level circulation in the South-Atlantic Ocean, *Prog. Oceanogr.*, *26*(1), 1–73, doi:10.1016/0079-6611(91)90006-8.

Pinedo-González, P., et al. (2015), Surface distribution of dissolved trace metals in the oligotrophic ocean and their influence on phytoplankton biomass and productivity, *Global Biogeochem. Cycles*, *29*, 1–19, doi:10.1002/2015GB005149.

Poulton, A. J., P. M. Holligan, A. Hickman, Y. N. Kim, T. R. Adey, M. C. Stinchcombe, C. Holeton, S. Root, and E. M. S. Woodward (2006), Phytoplankton carbon fixation, chlorophyll-biomass and diagnostic pigments in the Atlantic Ocean, *Deep Sea Res., Part II*, *53*(14-16), 1593–1610, doi:10.1016/j.dsr2.2006.05.007.

Quéroué, F., A. Townsend, P. Van der Merwe, D. Lannuzel, G. Sarthou, E. Bucciarelli, and A. Bowie (2014), Advances in the offline trace metal extraction of Mn, Co, Ni, Cu, Cd, and Pb from open ocean seawater samples with determination by sector field ICP-MS analysis, *Anal. Methods*, *6*(9), 2837–2847, doi:10.1039/c3ay41312h.

Ratten, J. M., J. LaRoche, D. K. Desai, R. U. Shelley, W. M. Landing, E. Boyle, G. A. Cutter, and R. J. Langlois (2015), Sources of iron and phosphate affect the distribution of diazotrophs in the North Atlantic, *Deep Sea Res., Part II*, *116*, 332–341, doi:10.1016/j.dsr2.2014.11.012.

Raven, J. A. (1988), The iron and molybdenum use efficiencies of plant growth with different energy, carbon and nitrogen sources, *New Phytol.*, *109*, 279–287, doi:10.1111/j.1469-8137.1988.tb04196.x.

Rees, A., J. Gilbert, and B. Kelly-Gerreyn (2009), Nitrogen fixation in the western English Channel (NE Atlantic Ocean), *Mar. Ecol. Prog. Ser.*, *374*(1979), 7–12, doi:10.3354/meps07771.

Rees, A. P., E. M. S. Woodward, and I. Joint (2006), Concentrations and uptake of nitrate and ammonium in the Atlantic Ocean between 60°N and 50°S, *Deep Sea Res., Part II*, *53*(14-16), 1649–1665, doi:10.1016/j.dsr2.2006.05.008.

Rijkenberg, M. J. A., R. J. Langlois, M. M. Mills, M. D. Patey, P. G. Hill, M. C. Nielsdóttir, T. J. Compton, J. LaRoche, and E. P. Achterberg (2011), Environmental forcing of nitrogen fixation in the Eastern Tropical and Sub-Tropical North Atlantic Ocean, *PLoS ONE*, *6*(12), doi:10.1371/journal.pone.0028989.

Riou, V., et al. (2016), Importance of N_2-fixation on the productivity at the North-Western Azores Current/Front System, and the abundance of diazotrophic unicellular cyanobacteria, *PloS ONE*, *11*(3), e0150827, doi:10.1371/journal.pone.0150827.

Rohardt, G., and A. Wisotzki (2013), *Physical Oceanography during POLARSTERN Cruise ANT-XXIX/1*, Alfred Wegener Inst., Helmholtz Cent. for Polar and Mar. Res., Bremerhaven, Germany, doi:10.1594/PANGAEA.817254.

Roussenov, V., R. G. Williams, C. Mahaffey, and G. A. Wolff (2006), Does the transport of dissolved organic nutrients affect export production in the Atlantic Ocean?, *Global Biogeochem. Cycles*, *20*, GB3002, doi:10.1029/2005GB002510.

Sarthou, G., et al. (2003), Atmospheric iron deposition and sea-surface dissolved iron concentrations in the eastern Atlantic Ocean, *Deep Sea Res., Part I*, *50*(10-11), 1339–1352, doi:10.1016/S0967-0637(03)00126-2.

Savoye, N., F. Dehairs, M. Elskens, D. Cardinal, E. E. Kopczynska, T. W. Trull, S. Wright, W. Baeyens, and F. B. Griffiths (2004), Regional variation of spring N-uptake and new production in the Southern Ocean, *Geophys. Res. Lett.*, *31*, L03301, doi:10.1029/2003GL018946.

Schlosser, C., J. K. Klar, B. D. Wake, J. T. Snow, D. J. Honey, E. M. S. Woodward, M. C. Lohan, E. P. Achterberg, and C. M. Moore (2014), Seasonal ITCZ migration dynamically controls the location of the (sub)tropical Atlantic biogeochemical divide, *Proc. Natl. Acad. Sci. U. S. A.*, *111*(4), 1438–1442, doi:10.1073/pnas.1318670111.

Shiozaki, T., T. Nagata, M. Ijichi, and K. Furuya (2015), Nitrogen fixation and the diazotroph community in the temperate coastal region of the northwestern North Pacific, *Biogeosciences*, *12*(15), 4751–4764, doi:10.5194/bg-12-4751-2015.

Sigman, D. M., K. L. Casciotti, M. Andreani, C. Barford, M. Galanter, and J. K. Böhlke (2001), A bacterial method for the nitrogen isotopic analysis of nitrate in seawater and freshwater, *Anal. Chem.*, *73*(17), 4145–4153, doi:10.1021/ac010088e.

Singh, A., M. W. Lomas, and N. R. Bates (2013), Revisiting N_2 fixation in the North Atlantic Ocean: Significance of deviations from the Redfield Ratio, atmospheric deposition and climate variability, *Deep Sea Res., Part II*, *93*, 148–158, doi:10.1016/j.dsr2.2013.04.008.

Snow, J. T., C. Schlosser, E. M. S. Woodward, M. M. Mills, E. P. Achterberg, C. Mahaffey, T. S. Bibby, and C. M. Moore (2015), Environmental controls on the biogeography of diazotrophy and Trichodesmium in the Atlantic Ocean, *Global Biogeochem. Cycles*, *29*, 865–884, doi:10.1002/2013GB004679.

Sohm, J. A., E. A. Webb, and D. G. Capone (2011a), Emerging patterns of marine nitrogen fixation. *Nat. Rev. Microbiol.*, *9*(7), 499–508, doi:10.1038/nrmicro2594.

Sohm, J. A., J. A. Hilton, A. E. Noble, J. P. Zehr, M. A. Saito, and E. A. Webb (2011b), Nitrogen fixation in the South Atlantic Gyre and the Benguela Upwelling System, *Geophys. Res. Lett.*, *38*, L16608, doi:10.1029/2011GL048315.

Staal, M., S. T. Lintel Hekkert, G. J. Brummer, M. Veldhuis, C. Sikkens, S. Persijn, and L. J. Stal (2007), Nitrogen fixation along a north–south transect in the eastern Atlantic Ocean, *Limnol. Oceanogr.*, *52*(4), 1305–1316.

Straub, M., D. M. Sigman, H. Ren, A. Martínez-García, A. N. Meckler, M. P. Hain, and G. H. Haug (2013), Changes in North Atlantic nitrogen fixation controlled by ocean circulation, *Nature*, *501*(7466), 200–203, doi:10.1038/nature12397.

Subramaniam, A., C. Mahaffey, W. Johns, and N. Mahowald (2013), Equatorial upwelling enhances nitrogen fixation in the Atlantic Ocean, *Geophys. Res. Lett.*, *40*, 1766–1771, doi:10.1002/grl.50250.

Torres-Valdés, S., V. M. Roussenov, R. Sanders, S. Reynolds, X. Pan, R. Mather, A. Landolfi, G. A. Wolff, E. P. Achterberg, and R. G. Williams (2009), Distribution of dissolved organic nutrients and their effect on export production over the Atlantic Ocean, *Global Biogeochem. Cycles*, *23*, GB4019, doi:10.1029/2008GB003389.

Turk, K. A., A. P. Rees, J. P. Zehr, N. Pereira, P. Swift, R. Shelley, M. Lohan, E. M. S. Woodward, and J. Gilbert (2011), Nitrogen fixation and nitrogenase (nifH) expression in tropical waters of the eastern North Atlantic, *ISME J.*, *5*(7), 1201–1212, doi:10.1038/ismej.2010.205.

Tyrrell, T., E. Marañón, A. J. Poulton, A. R. Bowie, D. S. Harbour, and E. M. S. Woodward (2003), Large-scale latitudinal distribution of Trichodesmium spp. in the Atlantic Ocean, *J. Plankton Res.*, *25*(4), 405–416, doi:10.1093/plankt/25.4.405.

Varela, M. M., A. Bode, E. Fernández, N. Gónzalez, V. Kitidis, M. Varela, and E. M. S. Woodward (2005), Nitrogen uptake and dissolved organic nitrogen release in planktonic communities characterised by phytoplankton size–structure in the Central Atlantic Ocean, *Deep Sea Res., Part I*, *52*(9), 1637–1661, doi:10.1016/j.dsr.2005.03.005.

Von Der Heyden, B. P., and A. N. Roychoudhury (2015), A review of colloidal iron partitioning and distribution in the open ocean, *Mar. Chem.*, *177*, 9–19, doi:10.1016/j.marchem.2015.05.010.

Voss, M., P. Croot, K. Lochte, M. Mills, and I. Peeken (2004), Patterns of nitrogen fixation along 10°N in the tropical Atlantic, *Geophys. Res. Lett.*, *31*, L23S09, doi:10.1029/2004GL020127.

Wasmund, N., U. Struck, A. Hansen, A. Flohr, G. Nausch, A. Grüttmüller, and M. Voss (2015), Missing nitrogen fixation in the Benguela region, *Deep Sea Res., Part I*, *106*, 30–41, doi:10.1016/j.dsr.2015.10.007.

Wilson, S. T., D. Böttjer, M. J. Church, and D. M. Karl (2012), Comparative assessment of nitrogen fixation methodologies, conducted in the oligotrophic north Pacific Ocean, *Appl. Environ. Microbiol.*, *78*(18), 6516–6523, doi:10.1128/AEM.01146-12.

Zhang, L., M. A. Altabet, T. Wu, and O. Hadas (2007), *Sensitive Measurement of NH4+ 15N/14N (δ15NH4+) at Natural Abundance Levels in Fresh and Saltwaters*, *79*(14), 5589–5595.